AIP | Applied Physics Letters

Sub-picowatt resolution calorimetry with a bi-material microcantilever sensor

Carlo Canetta and Arvind Narayanaswamy

Citation: Appl. Phys. Lett. **102**, 103112 (2013); doi: 10.1063/1.4795625
View online: http://dx.doi.org/10.1063/1.4795625
View Table of Contents: http://apl.aip.org/resource/1/APPLAB/v102/i10
Published by the AIP Publishing LLC.

Sub-picowatt resolution calorimetry with a bi-material microcantilever sensor

Carlo Canetta and Arvind Narayanaswamy[a)]
Department of Mechanical Engineering, Columbia University, New York, New York 10027, USA

(Received 18 December 2012; accepted 4 March 2013; published online 15 March 2013)

We have designed and fabricated bi-material microcantilevers with low conductance by minimizing the width and thickness of the cantilevers while keeping them suitable for detection with an optical deflection technique. The conductance of a cantilever is determined experimentally to be $330 \pm 20\,\mathrm{nWK^{-1}}$. Using this cantilever, we have measured less than 1 pW of heat flow through the cantilever. The thermal noise-limited resolution of the cantilever is expected to be ≈50 fW. Such cantilevers give us additional tools to probe thermal transport through nanostructures, especially through single molecules where picowatt-level sensitivity is necessary. © *2013 American Institute of Physics*. [http://dx.doi.org/10.1063/1.4795625]

Measurement of heat transport through single molecules has proven elusive thus-far in the study of nanoscale heat transfer. This measurement requires the ability to sense smaller magnitudes of heat transfer than what is currently possible. A microfabricated suspended device has proven to be a versatile platform for measurement of heat conduction through single nanowires.[1–4] It has been used extensively in measurements of heat conduction through carbon nanotubes and silicon nanowires, resolving power as small as 2 nW.[2] More sensitive measurements will allow for study of other interesting phenomena, including heat conduction through polymeric nanowires and the effects of molecular chain alignment which is believed to enhance thermal conductivity of polymers significantly compared to that of bulk polymer.[5] Such studies will have valuable implications for design of thermal interface materials. Looking further, while there have been measurements made on electrical conductivity of single molecules, heat conduction measurements on single molecules have proven inaccessible.[6–10] Estimates place the conductance of single molecules to be on the order of 10 pW/K.[6,11] Thus, if a stable temperature differential of 0.1 K across a molecule can be achieved, we may be able to probe single molecule thermal properties with a picowatt-resolution thermal sensor.

The bi-material microcantilever is a particularly sensitive calorimeter. A commercially available, triangular atomic force microscope (AFM) cantilever was used to measure power with resolution of 100 pW.[12] The resolution of a similar triangular cantilever was improved to 76 pW by optimizing thicknesses of the films which make up the cantilever.[13] By modulating the incident radiation at a frequency such that the limiting noise was reduced beyond low frequency $1/f$ noise, resolution was further improved to 40 pW.[14] Recently, a more complex microdevice consisting of a bi-material cantilever thermally isolated from its chip via long, thin beams was reported with resolution of ≈4 pW.[15]

In this letter, we show that the conventional bi-material cantilever can be modified, without sacrificing the ease of measurement via the optical deflection technique,[16] to enable sub-picowatt heat transfer detection. We propose a design in which the thickness and width of the cantilever are minimized to reduce the thermal conductance of the cantilever. We include in our cantilever design a wider area near the end of the cantilever large enough to accommodate a focused laser spot several micrometers in diameter. The formula for thermal conductance of a bi-material cantilever, G_c, can be written as

$$G_c = \frac{(kA)_{eff}}{L} = \frac{(k_1 t_1 + k_2 t_2)w}{L}, \tag{1}$$

where k and t are the thermal conductivity and layer thickness, respectively, w is the cantilever width, L is the length from the cantilever base to the point at which the laser is focused, and subscripts 1 and 2 denote the properties of the two materials. Silicon nitride cantilevers were fabricated with nominal dimensions $L = 85\,\mu$m, $w = 4\,\mu$m, $t_1 = 130$ nm. We have chosen silicon nitride as the material for the base cantilever because the thermal conductivity of silicon nitride is about five times lower than that of silicon, leading to a lower overall thermal conductance of the cantilever. Using the nitride cantilever base thickness of 130 nm and bulk material properties of silicon nitride and gold, we estimated the thickness of the gold layer for maximum thermal sensitivity to be ≈35 nm.[13] Using thin-film thermal conductivities of Si_3N_4 and Au ($2.2\,\mathrm{Wm^{-1}K^{-1}}$ and $85\,\mathrm{Wm^{-1}K^{-1}}$, respectively[17,18]), we calculate the thermal conductance of our cantilever to be 153 $\mathrm{nWK^{-1}}$. G_c was measured experimentally using a technique outlined by Narayanaswamy *et al.*[19] We measured the conductance to be $330 \pm 20\,\mathrm{nWK^{-1}}$. (All uncertainties quoted in this paper correspond to standard error unless otherwise noted.) The discrepancy between measured and calculated conductance can be attributed to uncertainty in the material properties, quality, and thickness of the thin films. A scanning electron microscope image of a fabricated cantilever is shown in Fig. 1(a).

Two lasers are used in the experiment. Figure 1(b) shows the optical apparatus by which the two lasers are focused onto a single cantilever. The setup is similar to that found in an atomic force microscope, with the addition of

[a)]Electronic mail: arvind.narayanaswamy@columbia.edu

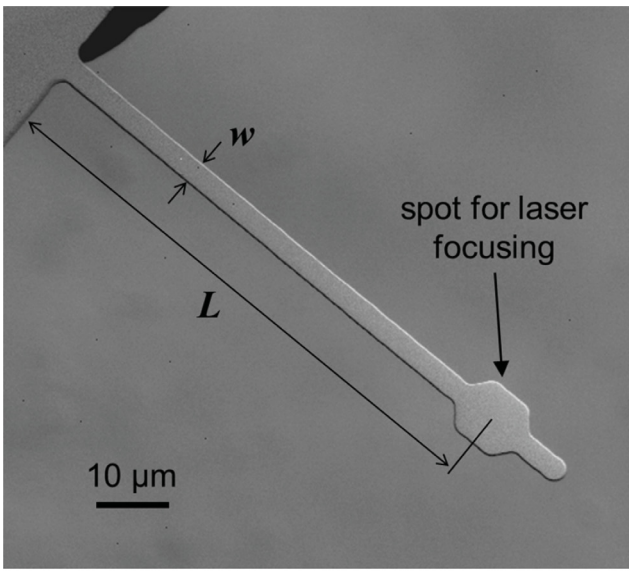

(a)

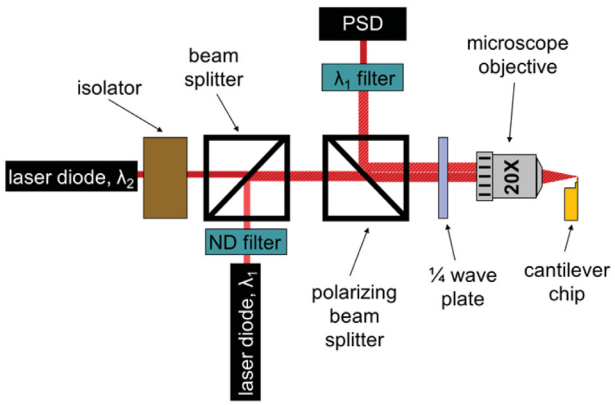

(b)

FIG. 1. (a) Scanning electron microscope image of a fabricated cantilever. (b) Optical apparatus used to focus two lasers onto the end of one cantilever. Isolator and polarization optics minimize reflected laser light returning to diode optical cavity. A neutral density (ND) filter allows for control of the power absorbed by the cantilever from the heating laser down to the sub-picowatt range.

polarization optics and beamsplitters for the purpose of introducing the second laser into the system and keeping the two lasers at near-normal incidence on the cantilever. The first laser is focused near the free end of the cantilever and its power is varied, thereby varying the heat flux to the cantilever. A neutral density filter placed in front of the heating laser allows us to control the power absorbed by the cantilever to sub-picowatt values. A second laser is focused on the same region of the cantilever and is used to sense the deflection of the cantilever. The position of the reflected spot from the second laser is monitored with a position sensitive detector (On–trak PSM2–10 with OT–301 amplifier), thereby recording deflection of the cantilever. The two lasers operate at different wavelengths (heating laser at $\lambda_1 = 670\,\text{nm}$, sensing laser at $\lambda_2 = 635\,\text{nm}$) so that the heating laser can be filtered out by using an appropriate filter before the position sensitive detector (PSD) and only the sensing laser spot is incident on the PSD. The entire apparatus is suspended on a passive vibration isolation platform inside a vacuum chamber with pressure <1.5 mPa.

The power resolution measurement is performed by modulating the power of the heating laser and using a lock-in amplifier to detect the deflection of the cantilever. Figure 2(a) shows the normalized PSD signal, which is proportional to cantilever deflection, versus the frequency of modulation of the heating laser, measured with two gain settings of the

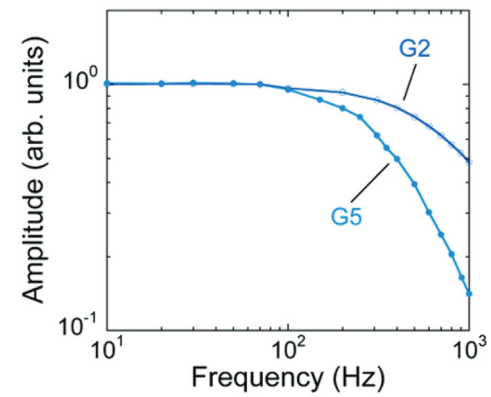

(a)

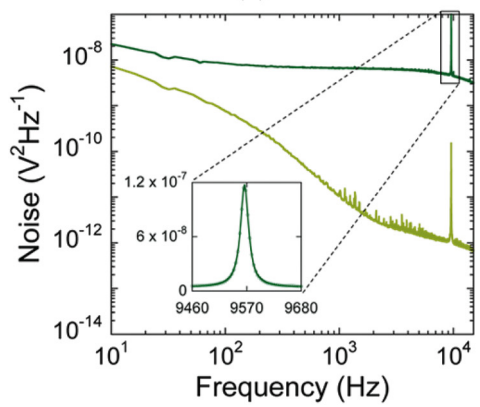

(b)

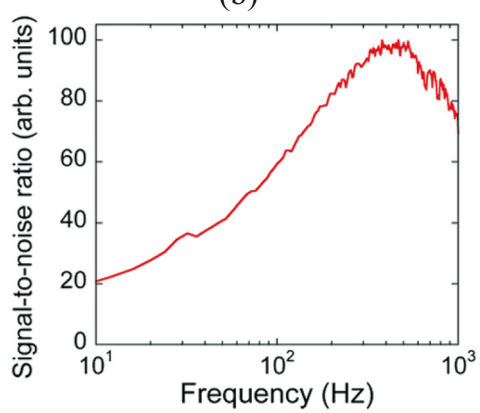

(c)

FIG. 2. (a) Position sensitive detector signal proportional to cantilever response versus heating laser frequency measured with lock-in amplifier. The y-axis is normalized by the signal in the low frequency limit. The lower curve is measured with the high gain setting of the PSD amplifier (G5 – bandwidth 310 Hz), the setting used in experiments. The upper curve is measured with a low gain setting which has a higher bandwidth (G2 – 15 kHz). (b) Power spectral density of the noise in the PSD signal. The lower curve is measured with the high gain setting. The upper curve is measured with the low gain setting which allows measurement of the first resonance unattenuated. Inset shows the noise near the first resonance frequency together with the fitted curve described in Eq. (4). (c) Signal-to-noise ratio computed from the corresponding signal and noise measurements made with the high gain setting. SNR peaks around 380 Hz.

PSD amplifier (G2 – low gain, G5 – high gain). In the upper curve, drop-off of the signal is due to the finite thermal time constant of the cantilever; the lower curve exhibits additional drop-off due to the lower bandwidth limit of the amplifier high gain setting. In the case where the cantilever is heated only at its end, the thermal time constant can be written as $\tau = \frac{wL}{2G_c}(\rho_1 C_1 t_1 + \rho_2 C_2 t_2)$, where C is the heat capacity and ρ is the density.[12] Using bulk values for material properties of gold and silicon nitride,[13] the time constant for our cantilevers is calculated to be ≈0.16 ms. The time constant can be determined experimentally as the inverse of that frequency at which the cantilever oscillation magnitude has decreased to 70% of the low frequency limit.[20] This frequency is found to be ≈560 Hz and the corresponding time constant 0.29 ms. Figure 2(b) shows the power spectral density of the noise in the detector signal, which includes contributions from the laser diodes as well as electrical and mechanical sources. Figure 2(c) shows the signal-to-noise (SNR) ratio for the high gain setting of the PSD amplifier. The modulation frequency of the heating laser was chosen to be the frequency at which the SNR is maximized (380 Hz in this case). The laser was modulated with a sinusoidal signal from a function generator (Agilent 33220A). The output signal from the function generator was used as the reference signal for the lock-in amplifier (Signal Recovery 7265).

In order to determine the heating laser power absorbed by the cantilever, an optical power meter (Thorlabs S2120B) was used to measure the laser power incident on, transmitted behind, and reflected from the cantilever.[19] Absorptivity could thus be calculated as the fraction of power incident on the cantilever that is not reflected or transmitted. Reflectivity and transmissivity were measured on two different days on which the experiment was run. The results of these measurements are presented in Table I. Notice that because the absorptivity is small, errors in the measured reflectivity and transmissivity significantly affect the perceived absorbed power. For comparison, reflectivity and transmissivity were similarly measured for the laser spot focused on a suspended structure with the same silicon nitride and gold layer thicknesses as the cantilever but with a much larger area. From these measurements, the reflectivity and transmissivity were measured to be 0.866 ± 0.003 and 0.065 ± 0.003, respectively, yielding an absorptivity of 0.069 ± 0.006. Reflection and transmission coefficients were also calculated for a four-layer medium (vacuum – gold – silicon nitride – vacuum) with the thicknesses of the gold and silicon nitride regions 35 nm and 130 nm, respectively. For the wavelength of the heating laser, 670 nm, refractive index, n, and extinction coefficient, κ, used were $n = 0.161$, $\kappa = 3.40$ for gold, $n = 2.02$, $\kappa = 0$ for silicon nitride.[21] Reflectivity, transmissivity, and absorptivity were calculated to be 0.847, 0.098, 0.055, respectively. Though we have confirmed that the focused laser spot appears visually to lie within the cantilever, a small fraction (<4%) is not incident directly on the cantilever. This explains the larger value of transmissivity in our measurements performed with the cantilever.

TABLE I. Cantilever absorptivity measurements performed during collection of two different data sets.

Data set	Reflectivity	Transmissivity	Absorptivity
1	0.831 ± 0.003	0.123 ± 0.001	0.046 ± 0.003
2	0.813 ± 0.002	0.131 ± 0.001	0.055 ± 0.002

The PSD signal proportional to the deflection of the cantilever due to power absorbed at the end is plotted in Fig. 3. For absorbed power <4 pW, a lock-in time constant of 100 s was used corresponding to measurement bandwidth of 1.2 mHz. The other points are measured with a time constant of 10 s corresponding to a 12 mHz bandwidth. A curve of the form $y = a\sqrt{x^2 + x_n^2}$ is fit to the full set of data shown in the inset of Fig. 3.[15] The term x_n corresponds to the noise equivalent power. To account for the error in measured absorptivity, a Monte Carlo simulation is performed whereby 1000 random absorptivity values are generated such that they obey a normal distribution with the same mean and standard deviation as in the measured absorptivity value. We use this distribution to generate 1000 data sets and perform the curve fitting as many times. The slope determined by this fitting method, a, is found to be 340 ± 20 nV/pW. The noise equivalent power, x_n, is found to be 0.9 ± 0.3 pW. The errors in the fitting parameters signify the interval in which 95% of the values lie. Using the measured thermal conductance of the cantilever, this corresponds to temperature resolution of $2.8 \pm 0.9\ \mu$K.

Our power measurement is limited by noise from the electronics, primarily the PSD amplifier, and from mechanical vibrations, primarily from the vacuum pump. If these sources of noise can be suppressed, the minimum power detectable by the cantilever sensor is limited by the thermal noise of the cantilever. The thermal noise-induced mean-squared amplitude fluctuations of the cantilever at frequency ν, denoted as $\langle \delta z^2(\nu) \rangle$, can be written as[22]

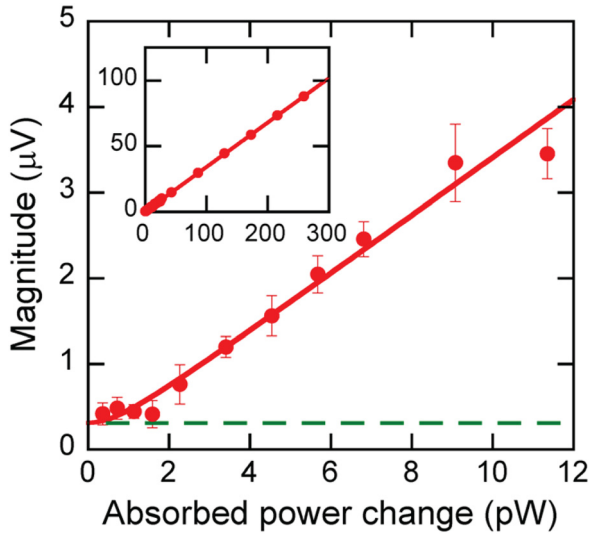

FIG. 3. Position sensitive detector signal corresponding to cantilever deflection plotted against change in power absorbed at the cantilever end. For absorbed power <4 pW (>4 pW), a lock-in time constant of 100 (10) s was used and each point represents the mean of 4 (10) individual measurements, and the error bars represent the standard error. The dotted line corresponds to the noise floor of the system for a time constant of 100 s (1.2 mHz measurement bandwidth). The noise floor is determined using the measured noise at 380 Hz from the noise spectrum presented in Fig. 2(b). The inset shows the cantilever response over a larger range of absorbed power.

$$\langle \delta z^2(\nu) \rangle = \frac{2}{\pi} \frac{k_B T B}{k_c \nu_k Q} \frac{1}{\left[1 - \left(\frac{\nu}{\nu_k}\right)^2\right]^2 + \left[\frac{\nu}{\nu_k Q}\right]^2}, \quad (2)$$

where B is the bandwidth of the measurement, k_c is the spring constant of the lever, ν_k is the natural resonant frequency, and Q is the quality factor of the cantilever at that resonance. We can write the spring constant, k_c, as

$$k_c = \frac{2}{\pi} \frac{k_B T Q}{\nu_k} \frac{B}{\langle \delta z^2(\nu_k) \rangle}. \quad (3)$$

The values of Q and ν_k can be determined by fitting a curve of the form

$$\langle V^2(\nu) \rangle = \frac{A_1}{\nu} + A_2 + \frac{\langle V^2(\nu_k) \rangle}{Q^2} \frac{1}{\left[1 - \left(\frac{\nu}{\nu_k}\right)^2\right]^2 + \left[\frac{\nu}{\nu_k Q}\right]^2} \quad (4)$$

to the measured mean-squared voltage fluctuation near the first resonant frequency.[23] The fitting parameters are A_1, A_2, Q, ν_k, and $\langle V^2(\nu_k) \rangle$; the fitted curve is shown in the inset of Fig. 2(b). From this fit, we find $Q = 486 \pm 2$, $\nu_k = 9565.60 \pm 0.03$ Hz and $\langle V^2(\nu_k) \rangle = (1134 \pm 3) \times 10^{-10}\,\mathrm{V^2 Hz^{-1}}$. A calibration of the detector signal performed by displacing the cantilever tip by a known distance with a piezoelectric transducer yields $\langle \delta z^2(\nu_k) \rangle = (124 \pm 4) \times 10^{-22}\,\mathrm{m^2 Hz^{-1}}$.[23] We then calculate the experimentally determined spring constant for our cantilever, $k_c = (107 \pm 4) \times 10^{-4}\,\mathrm{N m^{-1}}$. Returning to Eq. (2), we can find the noise due to thermal vibrations of the cantilever for the low gain setting of the PSD amplifier. Because we use the high gain setting for our measurements, we scale this value according to the transfer function relating the signal for the two gain settings, yielding the cantilever thermal noise limit as measured with the high gain setting of the PSD amplifier to be $(18 \pm 3) \times 10^{-14}\,\mathrm{V^2 Hz^{-1}}$. Using the slope, a, from the fit to our experimental results, we determine the thermal noise-limited power sensitivity of our cantilevers for a 1.2 mHz measurement bandwidth to be 44 ± 5 fW.

In summary, we have developed and fabricated ultrasensitive cantilevers capable of measuring absorbed power as small as less than 1 pW. With improvements to the apparatus, we should be able to approach cantilever thermal noise-limited power sensitivity of ≈50 fW. The demonstrated sensitivity of these cantilevers makes them a valuable tool for investigation of nanoscale thermal transport and potentially single molecule thermal transport.

This work has been partially supported by the National Science Foundation through Grants CBET–0853723, CHE–0641523, and CBET–1236165.

[1]P. Kim, L. Shi, A. Majumdar, and P. McEuen, Phys. Rev. Lett. **87**, 215502 (2001).
[2]L. Shi, D. Li, C. Yu, W. Jang, D. Kim, Z. Yao, P. Kim, and A. Majumdar, ASME Trans. J. Heat Transfer **125**, 881 (2003).
[3]D. Li, Y. Wu, P. Kim, L. Shi, P. Yang, and A. Majumdar, Appl. Phys. Lett. **83**, 2934 (2003).
[4]C. Yu, L. Shi, Z. Yao, D. Li, and A. Majumdar, Nano Lett. **5**, 1842 (2005).
[5]S. Shen, A. Henry, J. Tong, R. Zheng, and G. Chen, Nat. Nanotechnol. **5**, 251 (2010).
[6]A. Savin, M. Mazo, I. Kikot, L. Manevitch, and A. Onufriev, Phys. Rev. B **83**, 245406 (2011).
[7]T. Kodama, A. Jain, and K. Goodson, Nano Lett. **9**, 2005 (2009).
[8]X. Cui, A. Primak, X. Zarate, J. Tomfohr, O. Sankey, A. Moore, T. Moore, D. Gust, G. Harris, and S. Lindsay, Science **294**, 571 (2001).
[9]D. Porath, A. Bezryadin, S. De Vries, and C. Dekker, Nature **403**, 635 (2000).
[10]H. Fink and C. Schonenberger, Nature **398**, 407 (1999).
[11]D. Segal, A. Nitzan, and P. Hanggi, J. Chem. Phys. **119**, 6840 (2003).
[12]J. R. Barnes, R. J. Stephenson, C. N. Woodburn, S. J. O'Shea, M. E. Welland, T. Rayment, J. K. Gimzewski, and C. Gerber, Rev. Sci. Instrum. **65**, 3793 (1994).
[13]J. Lai, T. Perazzo, Z. Shi, and A. Majumdar, Sens. Actuators, A **58**, 113 (1997).
[14]J. Varesi, J. Lai, T. Perazzo, Z. Shi, and A. Majumdar, Appl. Phys. Lett. **71**, 306 (1997).
[15]S. Sadat, Y. Chua, W. Lee, Y. Ganjeh, K. Kurabayashi, E. Meyhofer, and P. Reddy, Appl. Phys. Lett. **99**, 043106 (2011).
[16]G. Meyer and N. M. Amer, Appl. Phys. Lett. **53**, 1045 (1988).
[17]M. Von Arx, O. Paul, and H. Baltes, J. Microelectromech. Syst. **9**, 136 (2000).
[18]J. Bourgoin, G. Allogho, and A. Hache, J. Appl. Phys. **108**, 073520 (2010).
[19]A. Narayanaswamy and N. Gu, J. Heat Transfer **133**, 042401 (2011).
[20]B. Kwon, M. Rosenberger, R. Bhargava, D. Cahill, and W. King, Rev. Sci. Instrum. **83**, 015003 (2012).
[21]E. Palik, *Handbook of Optical Constants of Solids* (Academic Press, 1985).
[22]D. Sarid, *Scanning Force Microscopy: With Applications to Electric, Magnetic, and Atomic Forces* (Oxford University Press, USA, 1994).
[23]N. A. Burnham, X. Chen, C. S. Hodges, G. A. Matei, E. J. Thoreson, C. J. Roberts, M. C. Davies, and S. J. B. Tendler, Nanotechnology **14**, 1 (2003).